Hindawi
Advances in Materials Science and Engineering
Volume 2022, Article ID 4861346, 8 pages
https://doi.org/10.1155/2022/4861346

Research Article

Studies on Mechanical Attrition and Surface Analysis on Heat-Treated Nickel Alloy Developed through Additive Manufacturing

B. Anush Raj,[1] J. T. Winowlin Jappes,[1] M. Adam Khan,[1] V. Dillibabu,[2] and N. Rajesh Jesudoss Hynes[3]

[1]*Department of Mechanical Engineering & Centre for Surface Engineering, Kalasalingam Academy of Research & Education, Virudhunagar, Tamilnadu, India*
[2]*Small Turbo Fan Section, Gas Turbine Research Establishment (GTRE), DRDO, Bangalore, India*
[3]*Department of Mechanical Engineering, Mepco Schlenk Engineering College, Sivakasi-626005, India*

Correspondence should be addressed to M. Adam Khan; adamkhanm@gmail.com

Received 19 October 2021; Revised 9 March 2022; Accepted 18 March 2022; Published 9 April 2022

Academic Editor: Alicia E. Ares

In this paper, the nickel-based superalloy SU718 is developed through the Direct Metal Laser Sintering (DMLS), an additive manufacturing process. Further, the material has been focused to study the effect of heat treatment and abrasive particle erosion. Two different heat treatment (HT) cycles are planed with ageing and annealing to enrich the metallurgical quality of the DMLS processed SU718 alloy. The heat treatment is performed with two different combinations of temperatures for annealing/solutionizing followed by ageing to improve the metallurgical properties. The influence of heat treatment on additively manufactured IN718 is imparting variations in the hardness, microstructure, and erosion resistance. Vickers hardness for as built, HT 1, and HT 2 of DMLS alloy is 264.15, 385.55, and 352.43 Hv; which has been increased for 45% for HT 1 and 33% for HT 2 from the as built DMLS alloy. After solutionizing, the grains are refined within the track boundary and the majority of the grains are homogenized. The air jet erosion test arrangement is used to conduct the study at a velocity of 250 m/s and impact angle of 90° at room temperature. The hardness of the treated samples has taken vital role to resist the erosion. The rate of erosion is higher for bare DMLS alloy whereas HT 1 has low erosion rate when compared with HT 2 and bare DMLS alloy. The erosion morphology of the samples was carried out by SEM images, and erosion mechanism is discussed. The ploughing and microcutting were found in all the impact angles, whereas erodent impingement is found in the bare DMLS alloy in additional. The good erosion resistance is observed for HT 1 DMLS alloy in all the impact angles.

1. Introduction

In the past decade, additive manufacturing is used to produce the prototype models, but nowadays researcher finds interest to manufacture components by additive manufacturing process due to its accuracy in dimension and can produce complex shape. The additive manufactured components are mainly used in the automobile, gas turbine, space, marine, and power generation application [1]. The additive manufacturing converts the three-dimensional virtual model of CAD data into two-dimensional layer and builds the object in the incremental form of layer by layer [2]. Mang et.al investigated on the additive manufactured IN718 and found that because of the highest cooling rate, the columnar grains are produced and built along the build direction. The samples fabricated by additive manufacturing process have anisotropic property [3]. The IN718 specimens fabricated by direct metal laser sintering (DMLS) were evaluated. IN718 alloy is the nickel-based super alloy which has good corrosion resistance and erosion resistance at high temperature; it is broadly used in aviation, aeronautical application, and marine and power generating application

[4]. The IN718 can be altered by proper heat treatment, and crystallographic changes can be made [5]. The alloy consists in major phases of gamma prime (γ'), gamma double prime (γ"), and delta (δ) phases and minor phases of laves and carbides. The chemical composition of Ni_3Nb is in the form of two structures, namely, tetragonal unit cell as γ" phase and orthorhombic unit cell as δ phase. Therefore, if the δ phase is increased, there is a decrease in the γ" phase which reduces the strength of the alloy [6].

Surface degradation is due to the wear and corrosion in gas turbine. The nickel-based super alloy used in the gas turbine provides good erosion resistance [7]. The degradation of the surface is caused due to the suspended particles in the liquid or gases. This suspended particles are rough irregular shapes and cause abrasion on the turbine blades. Due to the abrasion, the degradation of surface takes place and reduces the performance of the system. Also, it reduces the life of the system [8]. With the increase in hardness, the erosion resistance is increased [4]. Due to the solid particle erosion of the material, the surface damage and microstructure development also took place. The development of new microstructure on the eroded surface can change the erosion mechanism of the material [9].

The erosion mechanism of IN718 manufactured by DMLS process which is an additive manufacturing is not reported in any literature. The main objective of this paper is to understand the erosion mechanism of heat-treated IN718 manufactured by DMLS process with erodent velocity as constant and varying the impingement angle. The erosion scar is studied through macrograph of the sample.

2. Experimental Materials and Procedures

The IN718 powder of size of about 10–45 μm is used to fabricate, and the chemical composition of IN718 powder is shown in Table 1. The IN718 is fabricated with DMLS process (Model: EOS M280). The IN718 powders used of manufacturing are gas atomized with argon, and the grains are in spherical in size. The samples are manufactured in the horizontal orientation. The optimum parameter used for manufacturing is shown in Table 2. The average surface roughness of the fabricated samples is 2-3 μm.

The samples prepared by the DMLS process were subjected to different heat treatment. The heat treatment chart of the above heat treatment is shown in Figure 1, and corresponding details are furnished in Table 3. For HT 1, samples are solutionized at a temperature of 980°C for one hour followed by air cooling and double ageing at a temperature of 720°C for eight hours, furnace cooling to 620°C at the rate of 55°C/hr and maintained for eight hours, and cooled to room temperature by furnace cooling. For HT 2, the sample is homogenized at a temperature of 1100°C for two hours followed by air cooling and ageing at a temperature of 845°C for 24 hours and cooled to room temperature by furnace cooling. To reveal the microstructure, the samples are etched with solution composed of 16 ml H_2O + 4g $CuSO_4$ + 1 ml H_2SO_4 + 20 ml HCL.

In order to study the effect of heat treatment, the samples are metallurgically polished to measure the surface hardness. Based on the surface hardness, the metallurgical changes are predicted. To confirm the metallurgical changes, the samples are further subjected to X-ray diffraction analysis to read the changes in atomic level. The science of heat treatment with the peaks of X-ray diffraction and respective surface hardness is correlated. Subsequently, the air jet erosion testing machine (TR-470, Ducom, Bangalore, India) was used to investigate the erosion behavior of all test samples as per ASTM G76 standards. The erodent mix compressed air passes through the nozzle and strikes the sample which is placed on the angle sample holder at particular angle. The Alumina oxide particles size of 20–50 μm is widely used for the erosion testing. Table 4 shows the erosion test parameter used for evaluation. Therefore, the samples were cleaned with acetone and dried and weighted before erosion test and after erosion test in the electronic balance having an accuracy of ±0.01 mg. By using the change in mass, erodent flow rate (E_f), and discharge time (t), the erosion rate (E_r) of each sample is calculated using the equation as follows: erosion rate (E_r) = ($W_{initial}$−W_{final})/(E_f x t) where $W_{initial}$ is the weight of the sample before erosion test in g, Wfinal is the weight of the sample after erosion test in g, E_f is the erodent flow rate in g/sec, and t is the discharge time of erodent in sec.

The metallographic observation and crystallography of bare and heat treated DMLS samples are obtained by optical microscope and X-ray diffractometer (Bruker ECO D8 Advance), respectively. Scanning electron microscope (Make: Zeiss–FE SEM) attached with energy dispersive X-ray (EDAX) analysis is used to reveal the characterization of the eroded samples.

3. Results and Discussion

The microstructure of the bare DMLS sample observed on the building direction is shown in Figure 2(a). The laser beam scanning path is observed throughout the sample. The morphology of the metal pool appearance in the form of arc shape was found throughout the sample. In the overlap region, broad columnar grains are formed when it is seen in the building direction. The columnar grains represent hatch distance of the scanning path. This columnar region and dendrites are formed along the build direction. These dendrites in the DMLS samples make the sample anisotropy. To eliminate these nonequilibrium phases, the samples are repaired by suitable heat treatment process. After HT 1, the grains are refined within the columnar grain which is shown in Figure 2(b). Also, for HT 2, the grains are homogenized within the layer which is clearly shown in Figure 2(c). After heat treatment, the hardness is increased for 45% for HT 1 and 33% for HT 2 DMLS alloy. It is due to the repeated melting of metal powder and rapid solidification. While building a new layer, the reheating of existing layer may lead to produce metal carbide and it may invary at the end of DMLS process. It was observed that during solution treatment, γ'' and γ' phases are dissolved and the enrichment in δ phase was revealed. Figure 3 shows the XRD peak of the heat treated samples and the as built sample. After heat treating the HT1 DMLS alloy, the improvement of γ'' phase is due to

Table 1: The chemical composition of IN718 used for fabrication.

Element	C	Si	Co	Cu	W	Al	Ti	Mo	Nb	Cr	Fe	Ni
Wt. %	0.05	0.13	0.16	0.23	0.23	0.59	1.11	3.38	4.77	17.13	19.78	Bal

Table 2: Parameter for manufacturing IN718 samples in DMLS machine.

Parameter	Range
Power	285 W
Scan rate	970 mm/s
Hatching distance	0.15 mm
Layer thickness	40 μm
Beam diameter	80 μm

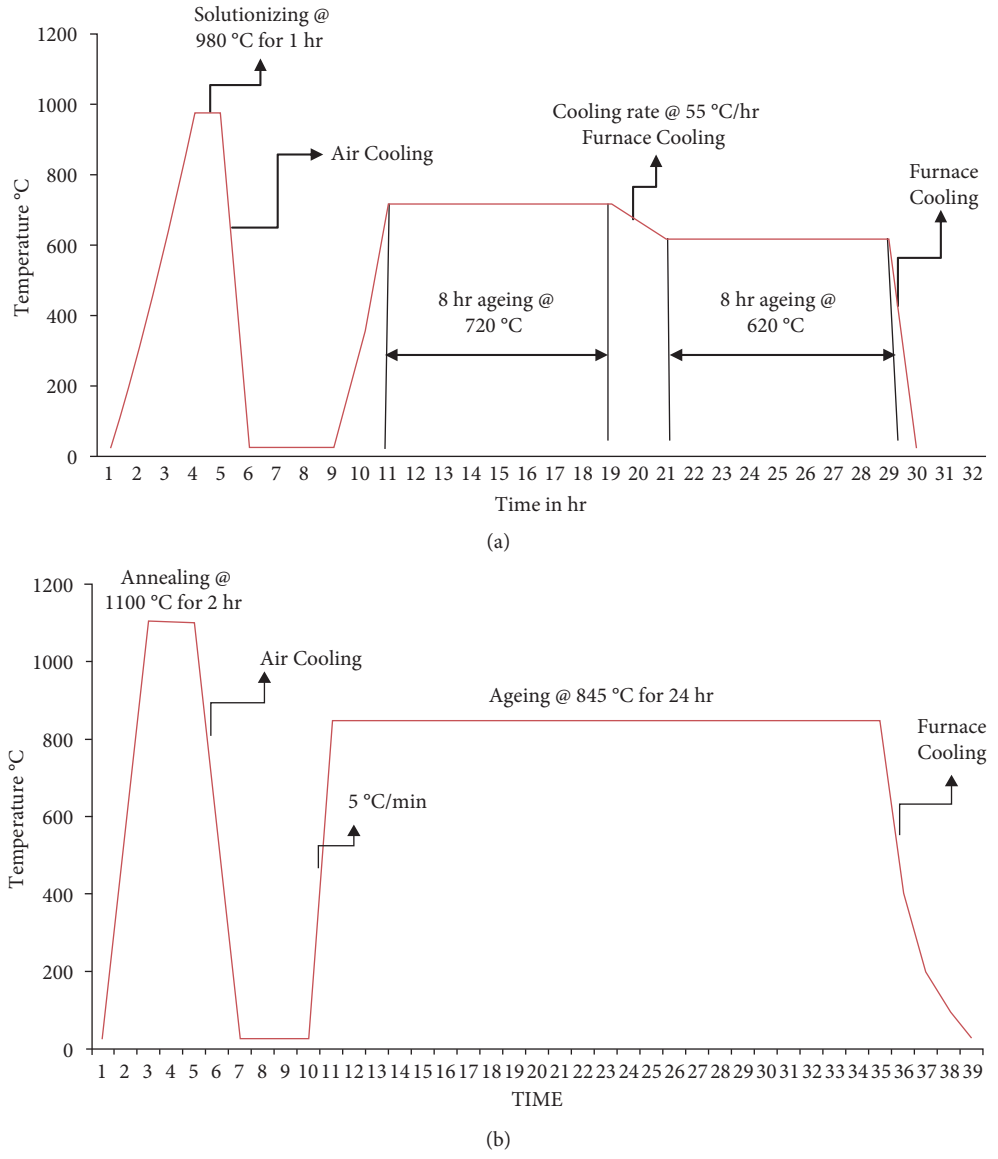

Figure 1: Heat treatment cycles for DMLS processed material: (a) HT 1 and (b) HT 2.

Table 3: Heat treatment variant.

Plan	Solutionizing	Cooling	Ageing	Cooling
HT 1	980°C/1 hr	Air cooling	720°C/8 hr and 620°C/8 hr	Furnace cooling
HT 2	1100°C/2 hr	Air cooling	845°C/24 hr	Furnace cooling

Table 4: Erosion test parameter for the proposed investigation.

Parameters	Range
Erodent material	Alumina
Particle size	50 micron
Particle velocity	250 m/sec
Erodent feed rate	5 g/min
Impact angle	90°
Nozzle diameter	1.5 mm
Test time	10 min

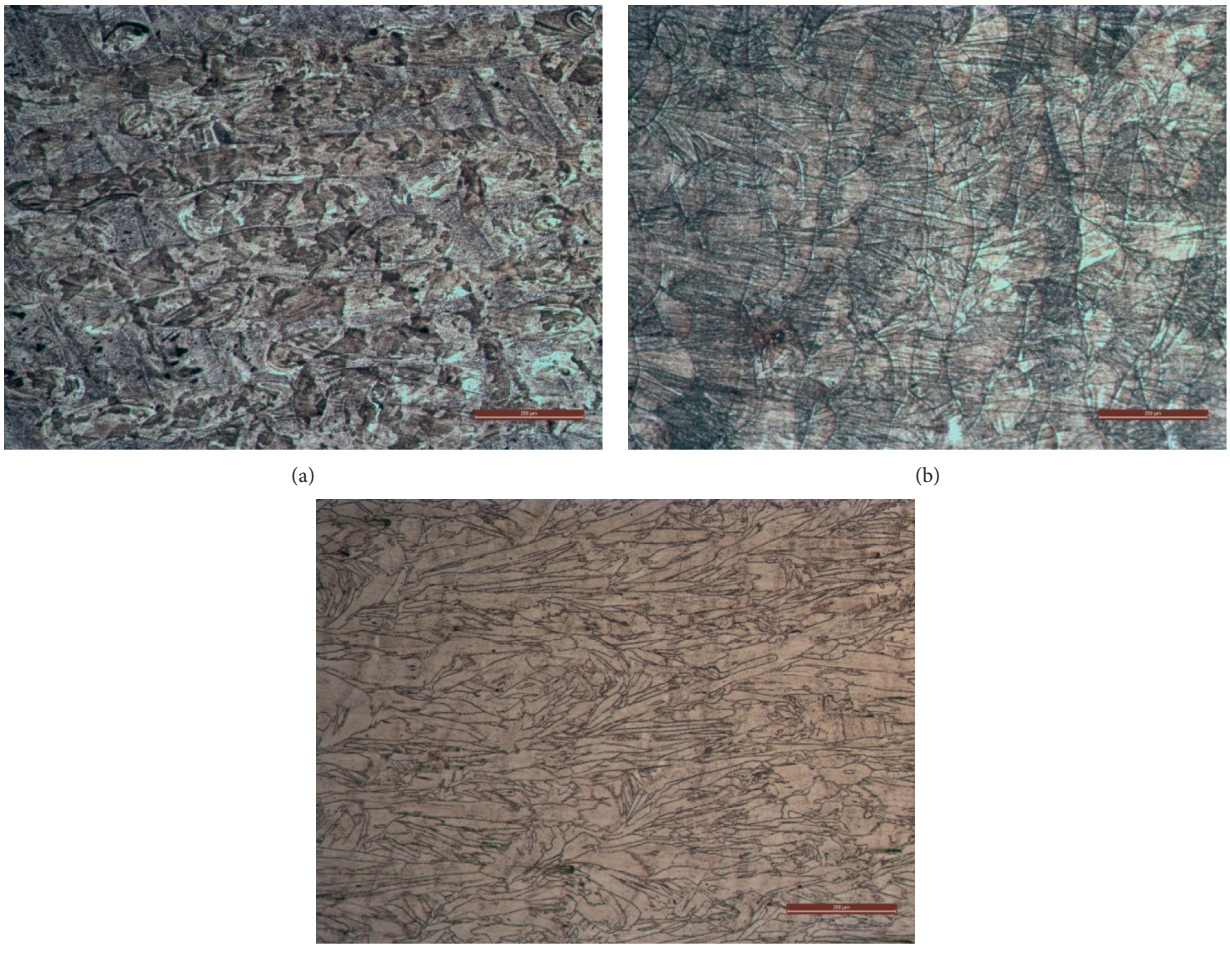

(a) (b) (c)

Figure 2: Optical microstructure of (a) as built, (b) HT 1, and (c) HT 2 DMLS alloy.

the segregation of Niobium elements in the form of BCT structure and γ' is formed due to the segregation of titanium and aluminum. In HT2 DMLS alloy, the δ phase is formed due to the segregation Niobium in the form of orthorhombic crystal structure; therefore, the γ" segregation is less which is clearly identified in the XRD graph. The effect of heat treatment on additive manufactured at 980°C has made metallurgical transformation by liquifying laves phase and releasing Nb atoms around the laves phase to improve the hardness [10]. Due to the uneven heat distribution and rapid cooling, the residual stress is caused. As a result of uneven heating and cooling process, distraction in metallurgical transformation may have an impact to pull down the strength in HT2 and base metal [11]. The reduction in γ'' and γ' phase and formation of δ phase lead to the reduction in hardness of alloy. Furthermore, Laves phase contains plenty of Mo, Ti, and Ni that may affect the strengthening of solid solution and decrease the number of γ'' and γ' phase which weakens the effect of precipitation. The presence of γ'', γ', and δ phase in the surface has increased the hardness with the HT1 sample. The metallurgical transformation of nickel alloy takes place at eutectic point (above 926°C), and it helps to form delta phase and their precipitates. In this research, it is evidently proved that the developed IN718 has completely

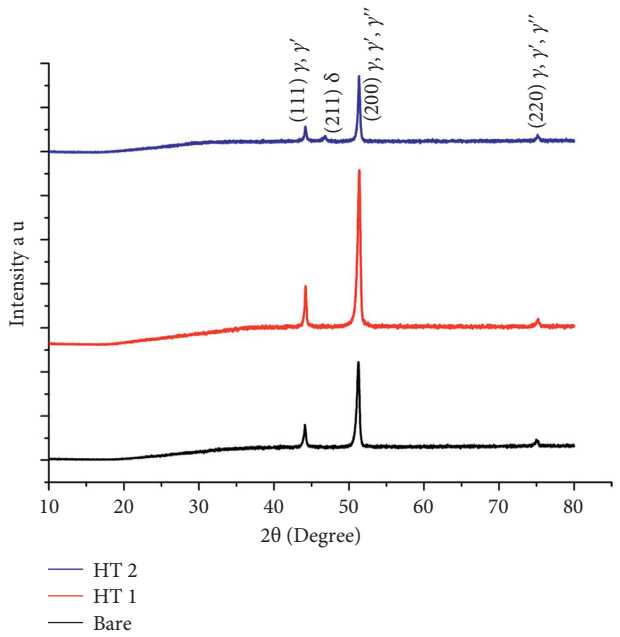

Figure 3: XRD peaks for the heat-treated sample and as built sample with phase diagram.

transformed into δ solvus during heat treatment (at 1100°C) and while ageing (at 845°C for 24 hours) the γ', γ'', and δ formation has taken place. In HT 1, the sample is double aged at 720°C and 620°C at 8 hours each, and the corresponding peak for the γ' and γ'' phase formation is strong. Therefore, the hardness of the alloy increased after heat treatment. The scale of Vickers hardness for bare, HT 1, and HT 2 DMLS alloy is 264.15, 385.55, and 352.43 Hv, respectively. The strength of the IN718 alloy mainly depends on the γ' and γ" of the alloy. The primary motive of the heat treatment is to fully solutionize the alloy and neglect the lave phase. During the fabrication process due to the rapid cooling, there is a formation of lave phase in the alloy which reduced the strength of the alloy. In HT 2 process, the sample is heat treated to 1100°C for 2 hrs which completely solutionized in the form of δ phase. In HT 1 process, the sample is heat treated to 980°C and double ageing at 720°C and 620°C where the lave phase is transformed in the form of γ' and γ" phase. Similar research in authentic phase transformation of additive built material is available in the literature for discussion [12].

Solid particle erosion test on metals mostly depends on the erosion test parameters such as flow rate of the erodent, velocity of the erodent, and impingement angle. In addition to the input process parameter, the quality of the erodent has also influenced over the erosion rate. Pure alumina is used an erodent having multiedges for the erosion study. Figure 4 shows the electron image of the alumina (erodent used for investigation) with similar dimensions and metallurgically qualified. The jet pressure used with high impact velocity strikes the surface of the DMLS processed alloy. Three samples per material grade are used for erosion studies. For a defined input process parameter, the erosion study is performed and weight loss is measured. Using the erosion rate formula for the recorded mass change, erosion rate is measured. Calculated erosion rate for the bare and the heat-treated DMLS alloy is given in Figure 5.

The sample tested at impact angle 90° exhibited the lowest erosion rate when compared with other impact angles. It is noted that the mass change in the erodent sample at perpendicular impingement is very meager. The mass change is in the range of 0.01 to 0.2 g for individual experiments. The bare DMLS sample exhibited the erosion rate of 5.02×10^{-4} Δg/g. The HT 1 and HT 2 DMLS alloy exhibited 3.81×10^{-4} Δg/g and 4.61×10^{-4} Δg/g rate of erosion. Heat-treated sample has good resistance towards erosion due to the metallurgical transformation. Presence of γ'', γ' and δ phase in the post processed alloy has increased bulk property. It has high strength to resist the erosion, and the intensity varies with respect the presence of precipitates (γ'', γ, and δ phase). The wear surface morphology and mechanism involved during the erosion are discussed in detail.

The erosion scar at the angle 90° for bare and heat-treated DMLS alloy is shown in Figure 6. The differences in the wear morphology due to impingement of the erodent over the surface of DMLS alloy for as built-bare, HT 1, and HT 2 (Figure 6(a)–6(c)) are elaborated in detail. The erosion scar diameter for the angle 90° impingement is very high for the HT 1 DMLS alloy and low in case of HT 2 DMLS alloy. The vertical force or normal force acts on the erodent which strikes the sample surface. The erosion resistance mainly depends on the hardness of the targeted surface, and the presence of hard precipitates resists the erosion. The similar results are obtained that the increase in hardness has increased the wear resistance of the material. To discuss in detail, the worn surface is investigated at higher magnifications.

The surface morphology of the worn surface is revealed with different wear mechanisms. Worn surface topography of the DMLS processed Inconel718 observed at higher magnification is given in Figure 7. The mechanical action of the solid particle erodent has impinged the surface and initiated plastic deformation on the bare DMLS alloy. Simultaneously, the repeated impingement of the erodent may strain harden the bare alloy, and when the strain hardening completed, the cracks are formed on the surface. The lip formation, crater, and ploughing are also observed on the surface of the heat-treated sample which is shown in Figures 7(c)–7(f). Fundamentally, the sliding of particle induces the surface to slide (shear) the surface, and the perpendicular impingement causes clinging effect. On the surface of heat-treated material, the crater and lip formation are noticed due to the continuous impact of erodent with multiedge which act as a spike during experimentation.

The improvement in the hardness of the heat-treated alloy improves the strain hardening of the sample and provides good resistance to erosion wear. It is also confirmed that the alumina solid particle after impingement found adhering to the worn surface. On continuous strike, the collision of alumina particle influences the erosion rate and the particle adheres to the surface with lip formation.

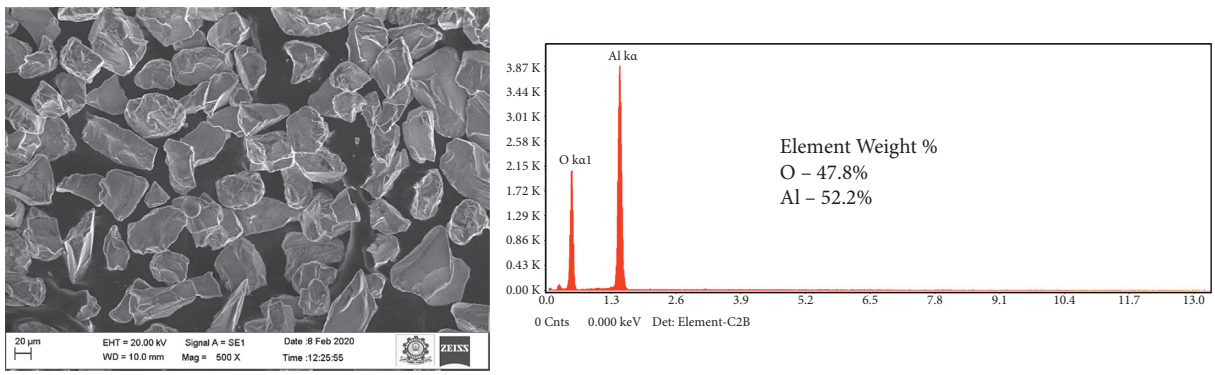

Figure 4: Electron image of the erodent particle with spectroscopic results.

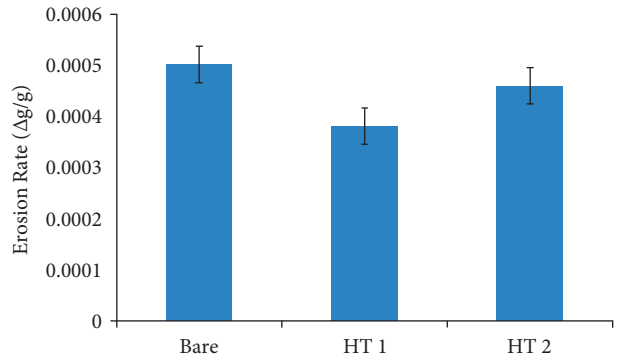

Figure 5: Erosion rate of the DMLS samples and hard particle impingement 90°.

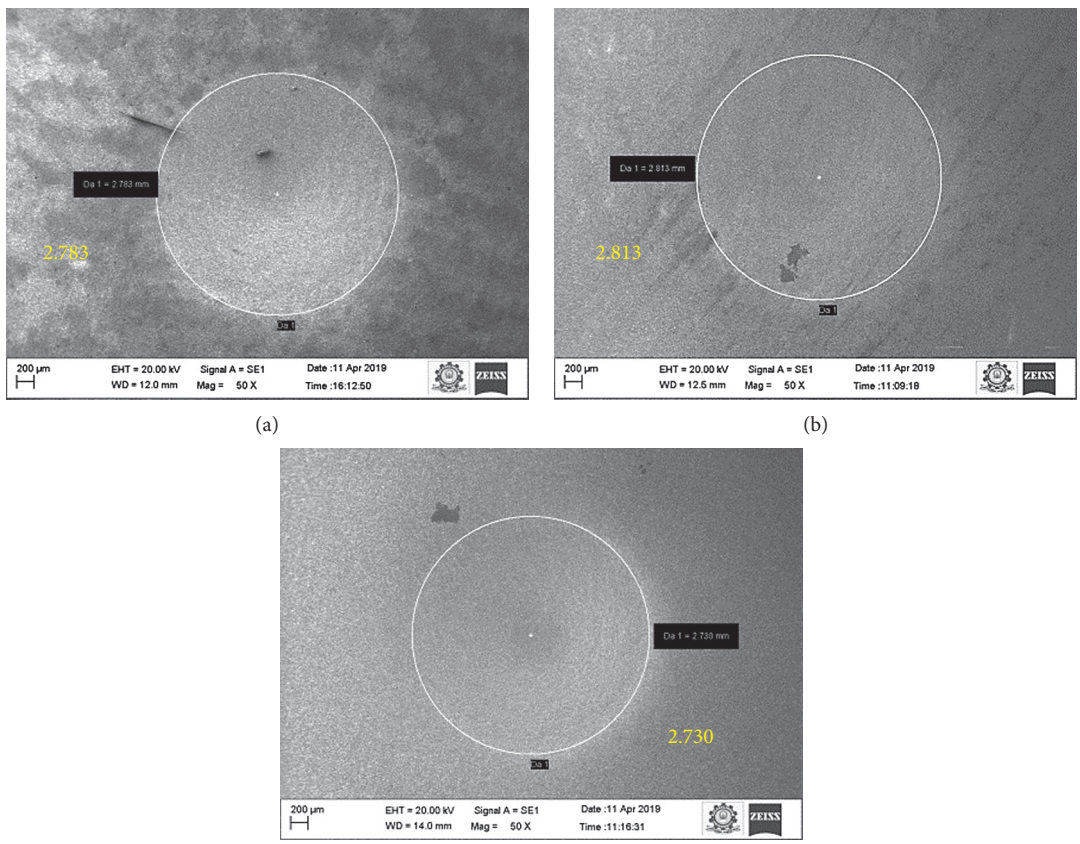

Figure 6: The diameter of erosion scar: (a) bare, (b) HT 1, and (c) HT 2 DMLS alloy.

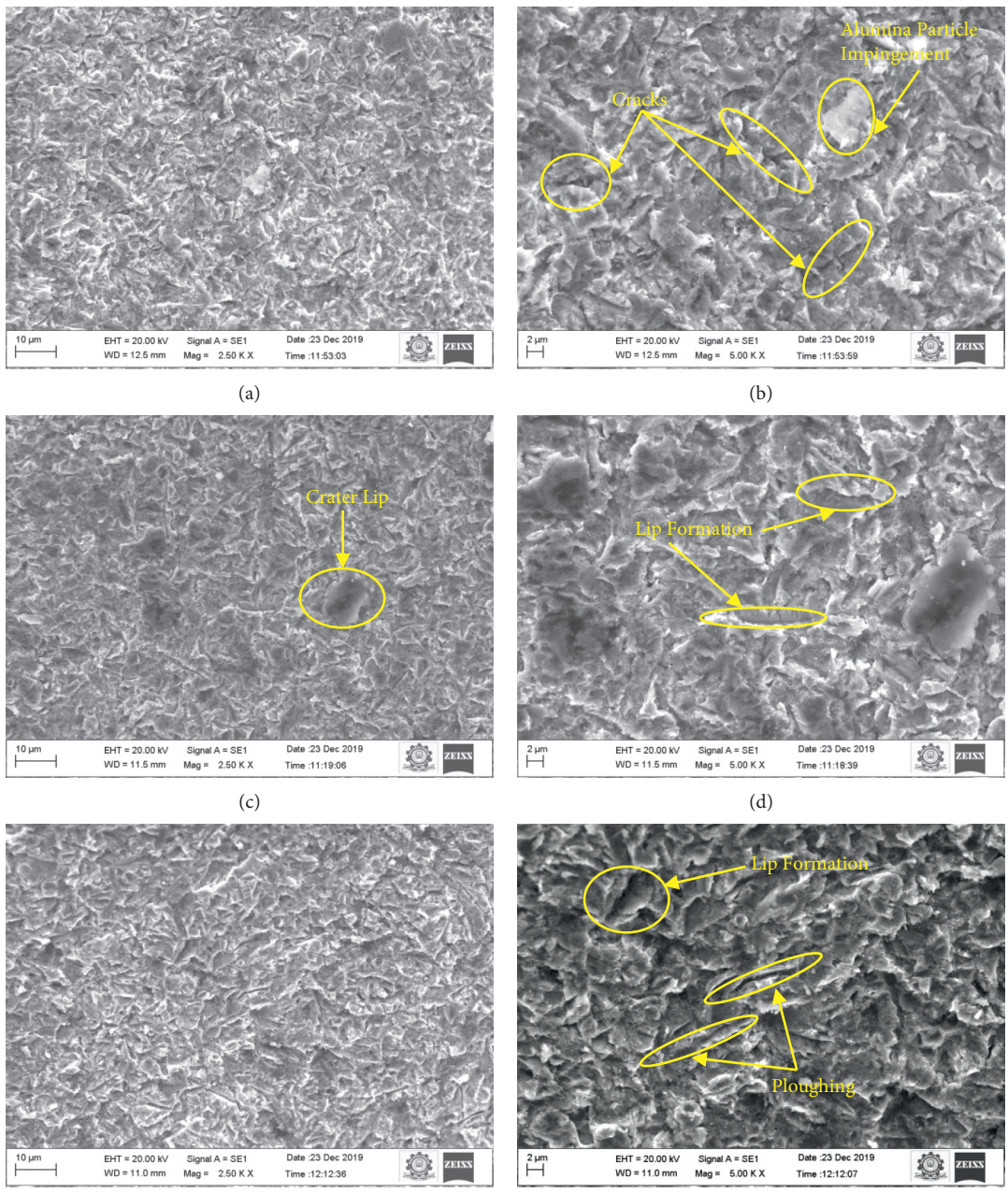

Figure 7: The higher and lower magnification of erosion morphology for the angle 90° for (a, b) Bare, (c, d) HT 1, and (e, f) HT 2.

Therefore, the metallurgical transformation due to isothermal heat treatment has highly influenced to increase the surface hardness of the DMLS processed alloy. In extension, the surface has high resistance towards erosion and controlled the material deterioration from severity in mechanical action of solid particle impingement.

4. Conclusions

The IN718 alloy is developed through DMLS process and followed by the different heat treatment plans. From investigation, following points found significant to justify the research findings:

(i) The heat treated DMLS alloy has significant changes in mechanical properties and metallurgical qualities. The wear resistance found increased with respect to increase in surface hardness. The built DMLS alloy has 264.15 Hv and expressively increased to 385.55 Hv for heat treated material. Vickers hardness found increased from 264.15 Hv to 385.55 Hv.

(ii) Concurrently, the built tracks found dissolved during heat treatment and the material revealed with austenitic phase. The carbides/dendrites in the built track reduced with annealing and complete phase transformation occurred with solutionizing.

It shows the metallurgical phase with achieved strength in change.

(iii) Indicating the erosion rate, annealed sample revealed with less in erosion rate (0.38 Δg/g) due to presence of partial carbide/dendrite structure. For the solutionized sample, erosion rate is average (0.46 Δg/g) compared with the as built DMLS alloy (0.5 Δg/g).

(iv) The common wear mechanism is revealed with lip formation and chipping due to hard particle impingement at perpendicular axis. However, the alumina particle striked on the surface found clinging with the as built material.

Therefore, it is recommended that the DMLS processed IN718 with annealing followed ageing has good mechanical properties, metallurgical strength, and high erosion resistance compared with solutionized sample and as built sample.

Data Availability

No data were used to support this study.

Conflicts of Interest

The authors declare that there are no conflicts of interest.

References

[1] I. Yadroitsev, L. Thivillon, P. Bertrand, and I. Smurov, "Strategy of manufacturing components with designed internal structure by selective laser melting of metallic powder," *Applied Surface Science*, vol. 254, no. 4, pp. 980–983, 2007.

[2] Ż. A. Mierzejewska, "Process optimization variables for direct metal laser sintering," *Advances in Materials Science*, vol. 15, no. 4, pp. 38–51, 2015.

[3] M. Ni, C. Chen, X. Wang et al., "Anisotropic tensile behavior of in situ precipitation strengthened Inconel 718 fabricated by additive manufacturing," *Materials Science and Engineering: A*, vol. 701, pp. 344–351, 2017.

[4] H. X. Hu, Y. G. Zheng, and C. P. Qin, "Comparison of Inconel 625 and Inconel 600 in resistance to cavitation erosion and jet impingement erosion," *Nuclear Engineering and Design*, vol. 240, no. 10, pp. 2721–2730, 2010.

[5] F. R. Caliari, N. M. Guimarães, D. A. P. Reis, A. A. Couto, C. De Moura Neto, and K. C. G. Candioto, "Study of the secondary phases in inconel 718 aged superalloy using thermodynamics modeling," in *Key Engineering Materials*vol. 553, pp. 23–28, Trans Tech Publications Ltd, 2013.

[6] C. Silva, M. Song, K. Leonard, M. Wang, G. Was, and J. Busby, "Characterization of alloy 718 subjected to different thermomechanical treatments," *Materials Science and Engineering: A*, vol. 691, pp. 195–202, 2017.

[7] H. Vasudev, P. Singh, L. Thakur, and A. Bansal, "Mechanical and microstructural characterization of microwave post processed Alloy-718 coating," *Materials Research Express*, vol. 6, no. 12, Article ID 1265f5, 2020.

[8] K. C. Wilson, G. R. Addie, A. Sellgren, and R. Clift, *Slurry Transport Using Centrifugal Pumps*, Springer Science & Business Media, Germany, 2006.

[9] Z. Li, J. Zhou, J. Han, and J. Chen, "Formation of cavitation-induced nanosize precipitates on the eroded surface for Inconel 718 alloy," *Materials Letters*, vol. 164, pp. 267–269, 2016.

[10] Z. Wang, K. Guan, M. Gao, X. Li, X. Chen, and X. Zeng, "The microstructure and mechanical properties of deposited-IN718 by selective laser melting," *Journal of Alloys and Compounds*, vol. 513, pp. 518–523, 2012.

[11] V. A. Popovich, E. V. Borisov, A. A. Popovich, V. S. Sufiiarov, D. V. Masaylo, and L. Alzina, "Impact of heat treatment on mechanical behaviour of Inconel 718 processed with tailored microstructure by selective laser melting," *Materials & Design*, vol. 131, pp. 12–22, 2017.

[12] D. Kong, C. Dong, S. Wei et al., "About metastable cellular structure in additively manufactured austenitic stainless steels," *Additive Manufacturing*, vol. 38, Article ID 101804, 2021.